

**Supplementary Materials**  
Electronic and Mechanical Characteristics of  
Stacked Dimer Molecular Junctions

**András Magyarkuti<sup>1</sup>, Olgun Adak<sup>2</sup>, Andras Halbritter<sup>1</sup>, Latha Venkataraman<sup>2,3</sup>**

<sup>1</sup> Department of Physics, Budapest University of Technology and Economics and  
MTA-BME Condensed Matter Research Group, 1111 Budapest, Budafoki ut 8., Hungary

<sup>2</sup> Department of Applied Physics and <sup>3</sup>Department of Chemistry, Columbia University, New  
York, NY 10027

**Contents**

- 1. Conductance histograms of the investigated molecules**
- 2. Analysis of noise sources**
- 3. Scaling of Flicker Noise in Dimer Junctions**
- 4. Determining the scaling exponent**
- 5. Constructing 2D Force Histograms**
- 6. Force spectroscopy measurement on 4,4''-p-diaminoterphenyl**
- 7. Force spectroscopy measurement on 4,4' Bipyridine**
- 8. References**

## 1. Conductance histograms of the investigated molecules

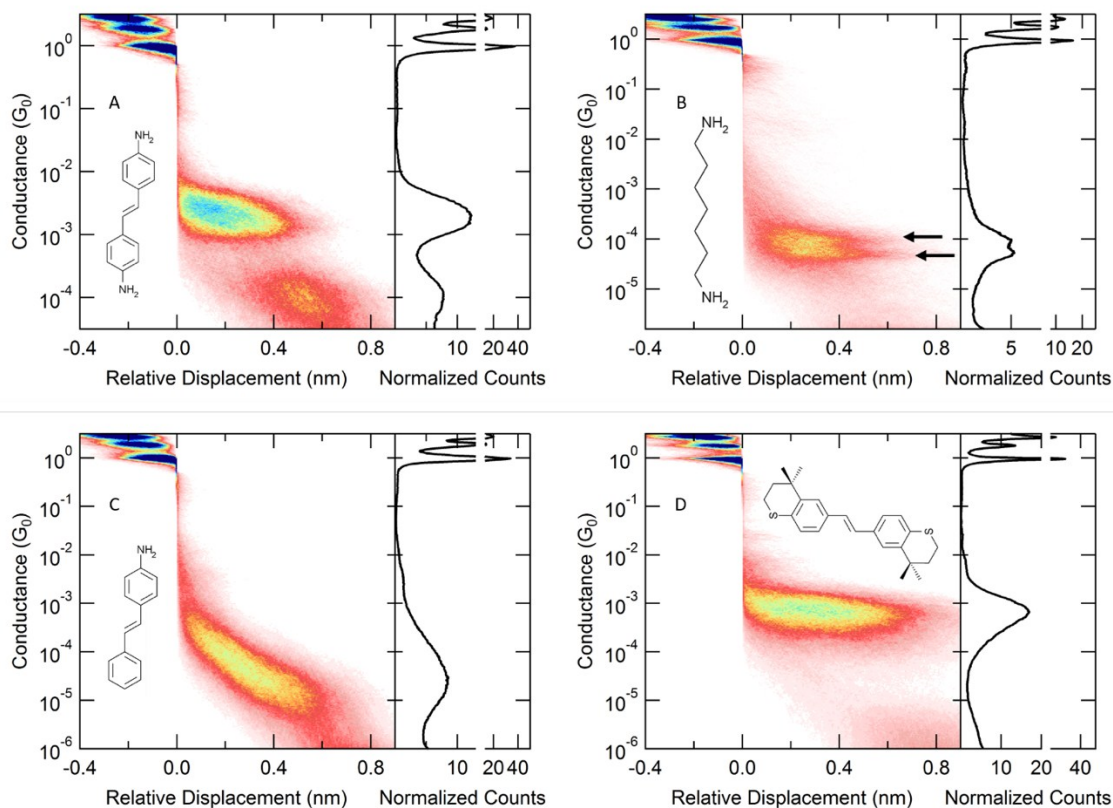


**Figure S1:** Conductance histograms and molecular structure of (A) 4,4'-diaminostilbene, (B) 1,7-diaminoheptane, (C) 4-aminostilbene, (D) (E)-1,2-bis(4,4-dimethylthiochroman-6-yl)ethane reproduced from *Batra et al.*<sup>1</sup>

## 2. Analysis of noise sources

During the experiment, we apply a bias voltage of 250 mV to the molecular junctions through a 100 k $\Omega$  series resistor. We measure the current flowing through the junction using a current amplifier (FEMTO DLPCA-200) with a gain set to  $10^6$ . To compare the noise measured on molecular junctions with the noise of the experimental setup, we replace the molecular junction with a 10 M $\Omega$  resistor (which is the typical value for molecular junction) and measure the output of the current amplifier using the same gain ( $10^6$ ) and bias voltage (250 mV). The resulting spectrum is shown in Figure S2 (black trace). At this gain setting, the input noise of the current amplifier dominates the measured noise ( $130 \text{ fA}/\sqrt{\text{Hz}}$  as specified by the manufacturer). To measure the thermal noise of the 10 M $\Omega$  resistor, we had to switch to a gain of  $10^{10}$ . The measured thermal noise was  $40 \text{ fA}/\sqrt{\text{Hz}}$  as shown in Figure S2. As a comparison, the averaged noise

spectrum of molecular monomer and dimer junctions for DAT and DAF monomer and dimer junctions are also shown. In every case, the noise measured in the 100-1000 Hz bandwidth is at least 2 orders of magnitude larger than the noise measured with 10 M $\Omega$  resistor.

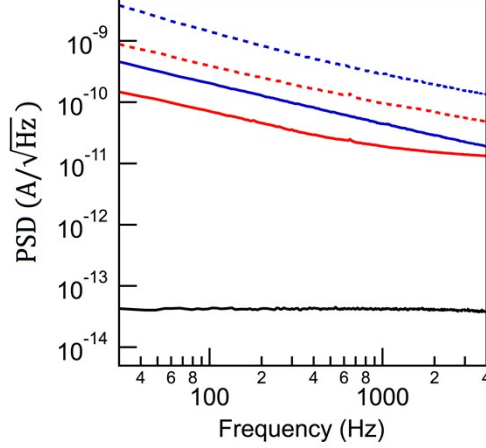


**Figure S2:** Current noise spectrum of the experimental setup. Thermal noise (black), DAF (blue) and DAT (red) molecular junction monomers (solid) and dimers (dashed).

### 3. Scaling of Flicker Noise in Dimer Junctions

We performed model calculations to gain better understanding on what determines the scaling exponent describing noise and conductance relation in case of dimer junctions. In our model, we consider two molecules: each molecule is bound to an electrode on one side, with coupling strength  $\Gamma_L$  and  $\Gamma_R$  respectively. Between the two molecules there is  $\delta$  inter-molecular coupling. The transmission function describes the probability of an electron with energy  $E$  to transfer from one electrode to the other across the junction. We model the transmission function of such a dimer junction with a single Lorentzian function:

$$T(E) = \frac{\Gamma_L \cdot \Gamma_R \cdot \delta^2}{((E - E_{Frontier})^2 + \Gamma_L \cdot \Gamma_R)^2}$$

where  $E_{Frontier}$  is the position of the frontier molecular orbital level relative to the Fermi level ( $E_F$ ). We take the limit, when  $E_{Frontier} \gg \Gamma_L \cdot \Gamma_R$  and the bias voltage applied across the junction is low, then conductance can be estimated as:

$$G = G_0 \cdot T(E_F) = G_0 \cdot \frac{\Gamma_L \cdot \Gamma_R \cdot \delta^2}{(E - E_{Frontier})^4}$$

Using a Monte Carlo simulation, we calculated conductance traces with generated noise. We assume that conductance noise originates from the fluctuations in the coupling strength parameters:  $\Gamma_L$ ,  $\Gamma_R$  and  $\delta$ . These parameters have both junction to junction variation and dynamic fluctuations. To simulate junction to junction variation, we assign a value to each of these parameters from a lognormal distribution. Electrode-molecule coupling is the same through-bond coupling on both sides, therefore we use the same lognormal distribution with a median of  $\Gamma_{Bond,0}$  and a standard deviation of  $\sigma_{Bond}$  for assigning values to  $\Gamma_L$  and  $\Gamma_R$ . Similarly, a value is assigned to  $\delta$  from a lognormal distribution with a median of  $\delta_{Space,0}$  and a standard deviation of  $\sigma_{Space}$ . Dynamic fluctuations account for the variation of the coupling strength parameters versus time. To simulate dynamic fluctuations, we add noise to the coupling parameters, the type of the added noise depends on the interaction described by the corresponding coupling parameter.

Thermally induced fluctuations change the separation between the molecules and introduce a noise in the coupling strength that is proportional to the average value of the coupling strength. To simulate dynamic fluctuations, we add noise to each of the coupling strength parameters ( $\Gamma_L^*$ ,  $\Gamma_R^*$  and  $\delta^*$ ). The type of the added noise, depends on the interaction described by the corresponding coupling parameter. For  $\Gamma_L$  and  $\Gamma_R$  describing through-bond coupling between electrode and molecule, we add a white Gaussian noise with zero mean and  $\sigma_{Noise,\Gamma}$  standard deviation. For  $\delta$ , which describes the through-space coupling, we add a Gaussian white noise with a standard deviation of  $\sigma_{Noise,\delta}$  multiplied by  $\delta/\Gamma_{Bond,0}$ . This results in a noise that is proportional to the value of the coupling strength  $\delta$ . We use the  $1/\Gamma_{Bond,0}$  factor to ensure that fluctuations of  $\delta$  are on the same scale as fluctuations of  $\Gamma_L$  and  $\Gamma_R$  when  $\delta = \Gamma_{Bond,0}$  and  $\sigma_{Noise,\delta} = \sigma_{Noise,\Gamma}$ . In Figure 2B, we show the result of such a Monte Carlo simulation generated using following parameters:  $\Gamma_{Bond,0} = 150 \text{ meV}$ ,  $\sigma_{Bond} = 0.4$ ,  $\delta_{Space,0} = 15 \text{ meV}$ ,  $\sigma_{Space} = 0.6$ ,  $\sigma_{Noise,\delta} = 20 \text{ meV}$ ,  $\sigma_{Noise,\Gamma} = 50 \text{ meV}$  and  $E = 1 \text{ eV}$ .

#### 4. Determining the scaling exponent

In order to determine the relation between flicker noise and conductance, we first sort traces based on the average conductance measured during the hold period. Monomer and dimer regions are determined based on the peak positions and widths on the 1D conductance histogram.<sup>2</sup> For every

selected trace, two quantities are calculated: power spectral density (PSD) and average conductance ( $G$ ). The relation between these quantities is described as:  $PSD \propto G^n$ , and we need to determine the value of  $n$ . Pearson's correlation coefficient is a measure of linear correlation between two variables:

$$r = \frac{\sum_i X_i Y_i - \frac{1}{n} \sum_i X_i \sum_i Y_i}{\sqrt{\left( \sum_i X_i^2 - \frac{1}{n} \left( \sum_i X_i \right)^2 \right) \left( \sum_i Y_i^2 - \frac{1}{n} \left( \sum_i Y_i \right)^2 \right)}}$$

We calculate the correlation coefficient,  $r$  between  $PSD / G^n$  and  $G$  as a function of  $n$ . Then we look for the value of  $n$ , where the correlation crosses 0. For this  $n$ ,  $PSD/G^n$  is independent of  $G$ , which means that this is the exponent describing the relation between noise and conductance.

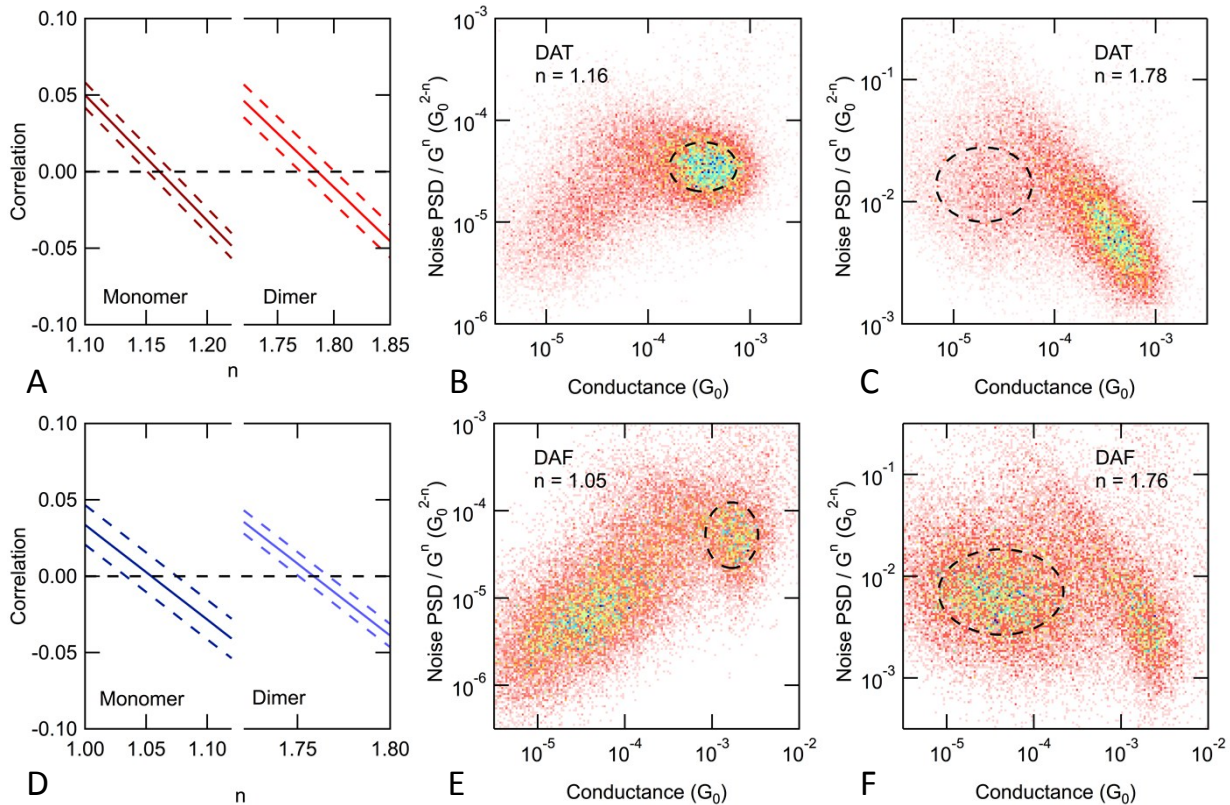


**Figure S3:** Analysis of the flicker noise measurements for DAT and DAF. (A, D) Correlation between noise  $PSD/G^n$  and  $G$  as the function of  $n$ , axis zoomed on the zero crossing. (B, E) and

(C, F) 2D histograms of noise  $PSD/G^n$  versus  $G$  for the monomer and dimer conductance regions respectively,  $n$  is set to the value, where correlation is zero.

The error of  $n$  can be estimated with the standard deviation of the correlation coefficient:

$$sr = \sqrt{\frac{1 - r^2}{N - 2}}$$

where  $N$  is the number of points in the datasets. SI-Figure S3A and D shows the zero-crossing point of the resulting  $r$  vs  $N$  along with the calculated error, which is only visible on a zoomed graph. It can be seen that error estimated this way is less than 0.02 in each case. This error does not account for the uncertainty of the conductance measurement.

SI-Figure S3B and S3C shows 2D histograms of  $PSD/G^n$  versus  $G$  for DAT molecule, with the scaling exponent  $n$  set to the value that gives a zero correlation. The overlaid contours are symmetric ellipses, indicating zero correlation between the two axes. (A tilted ellipse would indicate a correlation between the two axes).

## 5. Constructing 2D Force Histograms

A commonly used technique for extracting the average rupture force of a given junction structure is to create a force 2D histogram. First the measured conductance is used to determine the point of rupture. Then the force traces are aligned to this point both along the displacement and the force axis: each trace is offset to have zero displacement and zero force at the point of rupture. One can extract the average force curve from such a force histogram by fitting each vertical line with a Gaussian and overlaying the peak position on top of the 2D force histogram.<sup>3</sup> In case the traces were aligned at the final rupture event, the average rupture force can be determined by measuring the drop of the average force curve after the point of rupture. This method can be used to extract the rupture force of the dimer junctions but not the monomers. In the case of the monomers, once the junction breaks, a force loaded dimer junction is formed. Therefore the drop of the average force curve aligned at the monomer rupture point will be smaller than the actual force necessary to rupture these junctions. The other drawback of these force 2D histograms is that because of the force signal is not monotonic, the obtained average force curve is only valid in the close vicinity of the rupture point. Each trace exhibits a slightly different molecular step length, as a result the

overlaid traces quickly become blurred when moving away from the displacement point where the traces were aligned.

SI-Figure S4 shows 2D conductance and force histograms aligned at the point of rupture for metallic, monomer and dimer junctions. Due to the monotonic nature of conductance traces, all three features (single atom contact, monomer, dimer) can be identified on all the conductance 2D histograms and thus the evolution of the measured conductance can be inferred independently of the alignment point. On the contrary, average force curves extracted from force 2D histograms are only valid in the close vicinity of the alignment point. The only valid information is the amount the force signal drops when transitioning from one structure to the other. In order to capture the evolution of the force signal during the rupture process, this problem can be solved by creating a scaled 2D histogram through scaling and aligning each trace at multiple points. This way the actual displacement information is lost but the force information is retained throughout the junction elongation and rupture process.

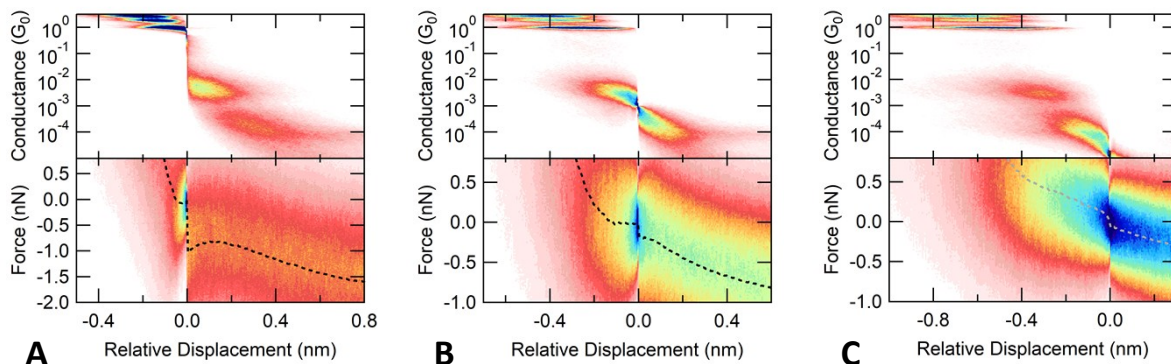


**Figure S4:** Two-dimensional conductance and force histograms for DAF, aligned at the rupture of (A) metallic, (B) monomer and (C) the dimer junction.

## 6. Force spectroscopy measurement on 4,4''-p-diaminoterphenyl

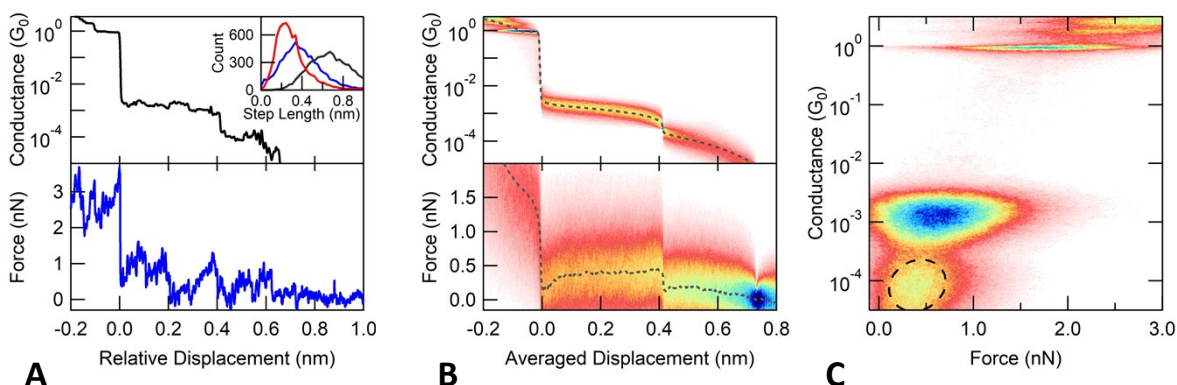


**Figure S5:** Force spectroscopy measurement of DAT. (A) Sample conductance and force trace. Inset shows the length distributions: entire molecular step (black), the monomer (blue) and dimer (red) junctions. (B) Scaled conductance and force histograms. (C) Conductance versus force histogram, the region of the dimer is fitted with 2D Gaussian, contours of the fit show correlation between conductance and force of 0.34.

### 7. Force spectroscopy measurement on 4,4' Bipyridine

Conductance measurements of 4,4'-Bipyridine (BP) have shown that it can exhibit a high and low conductance junction configuration. In contrast to DAT and DAF molecules in case of BP, both junction configurations correspond to a single molecule bridging the gap between the two electrodes.<sup>4, 5</sup> SI-Figure 6A shows the scaled 2D conductance and force histograms for BP junctions. Compared to DAT and DAF, rupture force of the final low conducting configuration is larger. During the elongation of the low conducting configuration the average rupture force is constant, in contrast for DAT and DAF the dimer junctions show a decrease in the measured force signal during elongation of the junction. SI-Figure 6B shows the conductance versus force 2D histogram where both the high and low conducting junctions exhibit uncorrelated conductance and force signals. The correlation coefficient obtained from 2D Gaussian fits is less than 0.02 in both cases. This is negligible to the correlation measured with DAT and DAF dimer junctions (around 0.3).

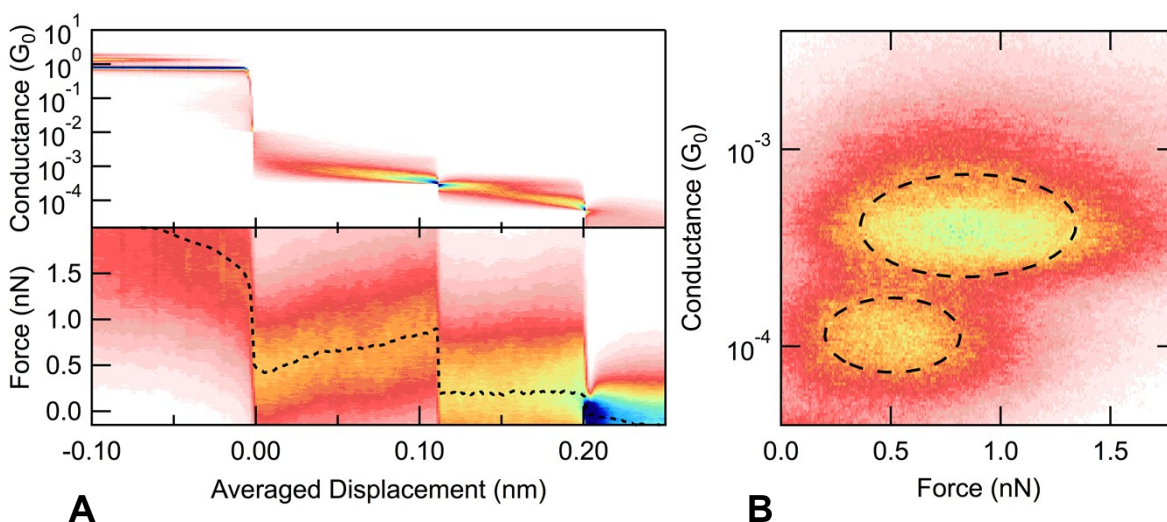


**Figure S6:** Force spectroscopy measurement of BP. (A) Scaled conductance and force histograms. (B) Conductance versus force histogram, both the high and low conducting regions are fitted with 2D Gaussian, the resulting correlation coefficient between conductance and force is less than 0.02 in both cases.

## 8. References

1. Batra, A.; Meisner, J. S.; Darancet, P.; Chen, Q.; Steigerwald, M. L.; Nuckolls, C.; Venkataraman, L. *Faraday Discussions*, **2014**, 174, (0), 79-89.
2. Adak, O.; Rosenthal, E.; Meisner, J.; Andrade, E. F.; Pasupathy, A. N.; Nuckolls, C.; Hybertsen, M. S.; Venkataraman, L. *Nano Lett.*, **2015**, 15, (6), 4143-4149.
3. Frei, M.; Aradhya, S. V.; Koentopp, M.; Hybertsen, M. S.; Venkataraman, L. *Nano Lett.*, **2011**, 11, (4), 1518-1523.
4. Quek, S. Y.; Kamenetska, M.; Steigerwald, M. L.; Choi, H. J.; Louie, S. G.; Hybertsen, M. S.; Neaton, J. B.; Venkataraman, L. *Nat. Nanotechnol.*, **2009**, 4, (4), 230-234.
5. Aradhya, S. V.; Frei, M.; Hybertsen, M. S.; Venkataraman, L. *Nat. Mat.*, **2012**, 11, (10), 872-876.